

## Simulation of the Complicated Patterns of Great earthquakes along the Nankai Trough: Part 2

HIROSE, Fuyuki<sup>1\*</sup>, MAEDA, Kenji<sup>1</sup>

<sup>1</sup>Meteorological Research Institute

### 1. Introduction

We have developed and improved a three-dimensional earthquake cycle model on the basis of the rate- and state-dependent friction law. Hirose and Maeda (2011, JpGU, SSJ) numerically simulated great earthquakes along the Nankai trough and produced some occurrence patterns such as (A) all region ruptured, (B) the Tokai region did not rupture occasionally, which is the case of the most recent Tonankai earthquake in 1944, (C) a part of or all part of the Nankai earthquake occurred two to five years after the Tonankai earthquake, and (D) long-term slow slip events (LSSE) in the Tokai region and Bungo channel occurred periodically. They distributed characteristic displacements ( $L$ ) and effective normal stress ( $\sigma$ ) heterogeneously considering locations of asperities of the 1944 Tonankai and 1946 Nankai earthquakes (Kikuchi et al., 2003, EPS; Murotani et al., 2007, SSJ), subducting ridges beneath the Tokai district (Kodaira et al., 2004, Science) and Hyuganada, the existence of water due to dehydration from the slab (Rice, 1992; Hirose et al., 2008, JGR). In addition, their model simulated also a pattern that only the Tonankai earthquake occurred. However, further inspection is necessary about the reliability of the model because we do not know that pattern in history.

By the way, it is suggested that the shallow region of the plate boundary slipped largely in the 2011 off the Pacific Coast of Tohoku Earthquake (Mw9.0, hereinafter 2011 Tohoku earthquake) (e.g., Yoshida et al., 2011, EPS). So far, it had classically been considered that aseismic slips had occurred constantly and coseismic slips had not occurred in the shallow region of the plate boundary off the Tohoku district (Uyeda and Kanamori, 1979, JGR). However, it was shown that this assumption was wrong by analysis of the 2011 Tohoku earthquake. In this study, taking above points into consideration, we tried to make a model that the shallow zone along the Nankai trough can sometimes slips largely when an earthquake occurs.

### 2. Method

As for the simulation method, we assumed that the shear stress on the fault obeys a rate- and state-dependent friction law derived from laboratory experiments (Rice, 1993, JGR). We used here the composite law (Kato and Tullis, 2001, GRL). Assuming that equilibrium between shear stress and frictional stress remains quasi statically, we numerically solved differential equations by the fifth-order Runge-Kutta method with an adaptive step-size control (Press et al., 1992). For simplicity, we considered that frictional parameters  $a$  and  $b$  depend only on depth and that the seismogenic zones for which  $(a - b)$  is negative is within the depth range from the Nankai trough to 30 km (cf. Hyndman et al., 1995, JGR). We assumed that  $a = 0.001$  for the entire depth range, and  $b = 0.0015$  for depths from 0 to 30 km. The characteristic displacement  $L$  was taken to be 2.0 m at shallower zone than 10 km; 0.5-1.0 m at subducted ridges beneath the Tokai region, Hyunagada, and intermediate region of the 1944 Tonankai and 1946 Nankai earthquakes; and 0.1 m elsewhere. By following the excess pore pressure model suggested by Rice (1992), ( $\sigma$ ) is given by  $rgz$  for  $z \leq 5.66$  km and 100 MPa for  $z > 5.66$  km, where  $z$  is depth,  $r = 1.8 \times 10^3$  kg/m<sup>3</sup>, and  $g = 9.8$  m/s<sup>2</sup>. The plate convergence rate we used along the Nankai trough was 6.5 cm/y in the western part of the study area, decreasing eastward from the Kii Peninsula to 1.5 cm/y in the eastern part of the study area (Heki and Miyazaki, 2001, GRL). Difference from the model of Hirose and Maeda (2011, JpGU, SSJ) is as follows: we set negative  $a-b$ , large  $L$  (= 2.0 m) in the shallower zone than 10 km.

### 3. Results and discussion

By setting above parameters, we made the model which shows complicated patterns. We simulated great earthquakes which ruptured up to shallow zones once in a few cycles by setting a barrier with large  $L$  at shallower zones than 10 km in depth.

Keywords: Nankai trough, great earthquake, simulation, characteristic displacement

## The possibility of seismic slip in the shallow and deep extensions of the seismogenic zone in the Nankai Trough

HYODO, Mamoru<sup>1\*</sup>, HORI, Takane<sup>1</sup>, BABA, Toshitaka<sup>1</sup>

<sup>1</sup>JAMSTEC seismo LP

In the 2011 Tohoku earthquake, it is generally accepted that the strong shakings and large tsunamis are excited by large slip near the trench axis from the analysis of various observation data (e.g. Fujiwara et al., 2011). Also along the Nankai trough, deposits of huge tsunami have been found from the coastal lakes (Okamura, 2011). However, such tsunamis were considered to be caused by concurrent ruptures of asperities laterally located in the seismogenic zone so far.

Recently, deep sea vessel, Chikyu obtained core data which implies the seismic slip might propagate to the up-dip end of the subduction interface off Kumano along the Nankai trough (Sakaguchi et al., 2011). This suggests that have occurred in the Nankai trough, not only the Showa-type eqs., great eqs. similar to the 2011 Tohoku. While, from model calculations of seismic cycle, by nesting asperity with different fracture energy (hierarchical asperity), both the massive earthquake ruptures up to the trench axis, and the normal earthquake which ruptures only seismogenic zone, may occur in different seismic cycles (Hori et al., 2009). From the above, in order to reconsider the seismic potential along the Nankai trough, we must reevaluate the possible variation of earthquakes there.

We apply the hierarchical asperity model to Nankai trough. To regard the conventional seismogenic zone as a small fracture energy zone,  $L=5\text{cm}$  is assumed at 10-20km depth. While due to large  $L=10\text{m}$  in the shallower region, the shallow plate boundary near the trough is modeled as large fracture energy zone.

As results, two types of earthquake with the different value of 0.4 in moment magnitude occur alternately. Hereafter we refer smaller earthquake as S eq., and larger one is L eq.. The interval between S eq. and L eq. is about 170 years, and next S eq. occurs 203 years after the occurrence of L eq..

The S eq. has large slip along the conventional seismogenic zone from Tokai to Hyuga-nada region, and becomes almost similar slip distribution to previously proposed Hoei model (Furumura et al., , 2011). In contrast, during L eq., coseismic slip extends to near the trough axis, and also extends to deeper region until 35km depth where the interpolate coupling is generally considered to be released by occurrences of VLF tremors.

As for vertical deformation expected from slip distributions, for both types of earthquake, the coast of Tosa Bay subsides about 1m similar to historical earthquake. In other regions, hinge line is also placed almost along the Pacific coastline for both eqs.. In Osaka Bay and Setouchi regions, the amount of subsidence in L eq. reaches several meters, since large slip area is extended to deeper than S eq. as mentioned above.

According to the calculations of the tsunami propagation which take the coseismic uplift and subsidence into account, in the case of L eq., tsunami heights of several meters are expected at Setouchi. These amounts of expected tsunami height are comparable to those of the historical records for Hoei event collected by Matsuura (personal communication). On the other hand, in S eq. with a slip distribution similar to the conventional Hoei model, significant tsunami does not reach the Setouchi and Osaka Bay, contradictory to Hoei tsunami data. In addition, the L eq. also predicts a large tsunami at Ryujin pond in Oita Pref. where deposits have been found due to a giant tsunami.

Accordingly, L eq. is consistent with the several observed data which implies the occurrence of huge earthquake along the Nankai trough. However, in L eq., large slip area is distributed from the trench to deeper VLF tremor zone. Hence, it is still unclear whether tsunamis in the pond Ryujin and the Setouchi areas are excited only by local slips such as near the trough, or by large slips over the entire plate interface. We should conduct additional studies to detect the origin of large tsunami and limit the possible models of Hoei type earthquake.

Keywords: Tohoku Earthquake, Nankai Trough, hierarchical asperity, crustal deformation, tsunami

## Correlation between the interplate coupling and the spherical oceanic lithosphere buckling at subduction zones

EGUCHI, Takao<sup>1\*</sup>

<sup>1</sup>National Defense Academy, Japan

We present a hypothetical model of mechanical stress change on the plate interface due to the slab age increases or decrease after the major spherical buckling.

Here, we assume that the absolute plate motion velocity of the overriding lithosphere is approximately zero at a subduction zone concerned.

Spherical tectonics suggests that, in the case of both edges of the single trench segment having been fixed with the mantle frame, if the slab age is gradually increasing or decreasing, the normal stress on the plate interface, i.e., interplate coupling, will be strengthened or weakened to some extent, respectively.

In the case of the abrupt increase or decrease in the slab age, the spherical slab segment might follow the mechanical buckling theory.

The buckling sequence of the trench segment(s) during morphological transformation is not like as a step function but as a gentle curve of some short period.

This is mainly because of the rheology response for the materials concerned, not only the slab segment itself but also the passive viscous flow regime within the surrounding upper mantle layer as well as the overriding lithosphere.

Keywords: interplate coupling, spherical shell buckling

## Large Scale Correlation of Interplate-type Earthquakes in Japan and a Speculative Interpretation

HAYASHINO, Tomoki<sup>1\*</sup>

<sup>1</sup>Neutrino Center, Tohoku University

After gigantic earthquake, 2011.3.11M9.0, it is frequently pointed out that activity of the earth's crust has been enhanced over the entire Japanese archipelago. Recent big earthquakes(EQs) which took place at faults in continental plates, such as Hyogo-Nanbu EQ(1995, M7.3), Tottori-seibu EQ(2000, M7.3), Niigata-chuetsu EQ(2004, M6.8), Noto-hanto EQ(2007, M6.9), Niigata-jyochuetsu-oki EQ(2007, M6.8), and Iwate-nairiku-nanbu EQ(2008, M7.2), which are extensively distributed on a large scale over Japan, are sometimes discussed in relation to interplate-type EQ 3.11M9.0.

In the present study, the author has investigated long range(i.e., large scale) correlation between Ibaraki-oki interplate-type earthquakes and Hyuganada ones from 1930 to 2010, using the seismic intensity catalog archived by the Meteorological Agency of Japan. Here, earthquakes in two areas are considered to be independent in general, because Ibaraki prefecture is about 1000km distant from Miyazaki prefecture, and the former is belonging to North-American plate, while the latter is located on Firi-pin-sea plate.

The following results are obtained.

(1) Average event rate between 1930 and 2010 are 0.81 times/year(=4.1/5y) for Ibaraki-oki  $M > 5.7$  earthquakes, and 0.45/y(=2.3/5y) for Hyuganada  $M > 5.5$  ones.

Both areas seem to show similar time variability, though low statistics.

(2) Define H(high) phase as well as L(low) phase in Ibaraki-oki as the followings,

H phase ; period with 5 or more  $M > 5.7$  earthquakes per 5 years

L phase ; period with 4 or less  $M > 5.7$  earthquakes per 5 years

Hyuganada has the following  $M > 5.5$  earthquakes in each phase of Ibaraki-oki,

Ibaraki-oki Hyuganada/5years

H phase ; 4.3 +/- 1.0

L phase ; 1.5 +/- 0.4

Although the above correlation is not robust in the present statistics, long range correlation of interplate-type earthquakes would be implied.

In a talk, the author will propose a model which is very speculative, to understand large scale correlation.

Keywords: interplate-type earthquake, time variability, long range correlation

## Relations of rupture area of great Kurile earthquakes estimated by tsunami waveform analysis

IOKI, Kei<sup>1\*</sup>, TANIOKA, Yuichiro<sup>1</sup>

<sup>1</sup>ISV, Hokkaido University

The Pacific plate subducts about 8cm per year under the Kurile Islands, so many great earthquakes occurred in the Kurile subduction zone. On 13 October 1963, great Kurile earthquake (Mw 8.5, Mt 8.4) occurred off the Etorofu Island. This event was an underthrust earthquake. The epicenter of the 1963 earthquake is located at 44.8N, 149.5E, depth = 60 km. Also the largest aftershock (Ms 7.2, Mt 7.9) occurred on 20 October 1963. This aftershock generated an unusually large tsunami relative to the size of the seismic waves. The epicenter of the 1963 aftershock is located at 44.7N, 150.7E, depth = 10 km. The 2006 Kurile earthquake occurred northeast of the 1963 Kurile earthquake. The epicenter of the 2006 earthquake is located at 46.6N, 153.2E, depth = 30 km. To examine whether seismic gap exist between 1963 and 2006 earthquakes and to understand source processes of the 1963 main shock and the largest aftershock, slip distributions of the 1963 great earthquake and the largest aftershock were estimated using tsunami waveforms recorded at tide gauges along Pacific Ocean and Okhotsk Sea coast. In the case of the main shock, the total seismic moment was estimated to be  $2.4 \times 10^{21}$  Nm (Mw 8.2). The 2006 earthquake occurred just next to the 1963 earthquake and no seismic gap exists between source areas of the 1963 and 2006 earthquakes. In the case of the largest aftershock, large slip amounts were found at the shallow plate interface near the trench. This largest aftershock was a tsunami earthquake. The seismic moment was estimated to be  $1.0 \times 10^{21}$  Nm (Mw 7.9). On 6 November 1958, the great Etorofu earthquake (Mw 8.3) occurred southwest of the 1963 Kurile earthquake. The epicenter of the 1958 earthquake is located at 44.4N, 148.6E, depth = 80 km. The 1958 great earthquake was defined as a slab event. In this study, dip, depth, slip amount of the earthquake were estimated by tsunami waveforms analysis. Strike and rake of the fault model were fixed. We found that a slab earthquake model of dip = 40 degree, depth = 37.5 km best fit observed and computed tsunami waveforms. The seismic moment estimated by tsunami waveform inversion was  $1.7 \times 10^{21}$  Nm (Mw 8.1). About the 1969 Hokkaido-Toho-Oki earthquake, the earthquake (Mw 8.2) occurred southwest of the 1963 earthquake. The epicenter of the 1969 earthquake is located at 43.2N, 147.5E, depth = 33 km. The 1969 event was an interplate earthquake with the same type event as the 1963 event, but the 1958 event was a slab earthquake. Slip distribution of the 1969 earthquake was estimated from tsunami waveform inversion to investigate relations of locations of the 1969 and 1963 and 1973 earthquake. 1973 Nemuro-Oki earthquake is underthrust earthquake and the epicenter of the earthquake is located at 43.0N, 146.0E, depth = 40 km. The seismic moment of the 1969 earthquake was estimated to be  $1.1 \times 10^{21}$  Nm (Mw 8.0). The 1963 earthquake and 1973 earthquake occurred northeast and southwest of the 1969 earthquake and no seismic gap exists between source areas of these earthquakes.

Keywords: tsunami, great earthquake, Kurile trench

## M=9.0 Tohoku Earthquake and tsunami; a new interpretation

MARUYAMA, Shigenori<sup>1\*</sup>

<sup>1</sup>Tokyo Institute of Technology

### M=9.0 Earthquake:

M=9.0 earthquake occurred at 3.11, 2011 and its unusually large magnitude has been discussed since then. Here I propose a different process from the Benioff plane origin, but along a spray-fault that destroyed the fore-arc region. This is a process of tectonic erosion to break the hanging wall of overriding lithosphere, and transport it into deep mantle, presumably in mantle transition zone to develop the 2nd Continents through time.

Origin of spray faults is a manifestation of physically unstable triangular region between material boundary (trench) and physical boundary (spray fault). The tightly connected Benioff thrust dragged down the frontal part of overriding plate to reactivate the spray fault to form M=9.0 earthquake.

### Tsunami:

The spray fault occurs right below the trench-slope break which is a turning point of slope change from shallow to deep trench inner wall. Right above the fault, sedimentary basin is present. Huge-scale submarine landslide occurred by the collapse of fulfilled sedimentary basin, which caused the tsunami off Sendai.

The river drainage system on NE Japan is remarkably different from SW Japan. Two major rivers, one from the north and another from the south to transport the eroded sediments on NE Japan meet in Sendai to carry them in the sedimentary basin off Sendai. This basin will periodically collapse, say, every 1000 years, to trigger tsunami.



## Have the prior afterslip areas been barriers to the 2011 Tohoku earthquake?

KAWASAKI, Ichiro<sup>1\*</sup>

<sup>1</sup>DMUCH, Ritsumeikan U. and TRIES

Common features of rupture expanding process models of the 2011 Tohoku earthquake (eg, Koketsu et al., 2011; Shao et al., 2011; Suzuki et al., 2011; Yoshida et al., 2011; Yagi and Fukahata et al., 2011; Ide et al., 2011) can be summarized as follows

(1) major rupture of slip of 40m to 50m has continued to expand for around 1 minute in an area between N37.5 to N39 longitudinal lines under the continental shelf.

(2) the major rupture to the north has stopped at N39, where was the southern boundary of the afterslip area associated with the 1992 Sanriku-oki earthquake (Mw6.9).

(3) the major rupture to the south has started to cross N39, where was the northern boundary of the afterslip area associated with the 2008 Fukushima-oki earthquake (Mw6.9), while seismic slip has been a few meters, one order smaller than the major rupture.

Questions arise. Why have the major rupture been blockaded at N39? Why has the major rupture been delayed to cross N37.7?

We remember that some afterslips were discovered in Tohoku-oki area in 1990's and 2000's, which are mapped in the figure below. On the other hand, based on numerical simulations invoking with the frictional law of fault slip, Yoshida and Kato (2003) segmented slip area into four modes (K1) - (K4) as a function of (a-b) and  $P_n$  (a-b is friction parameter and  $P_n$  is the stress normal to a slip plane) and  $l$  (inverse of fault stiffness) as

(K1)  $a-b < 0$ ,  $l$  small : asperity.

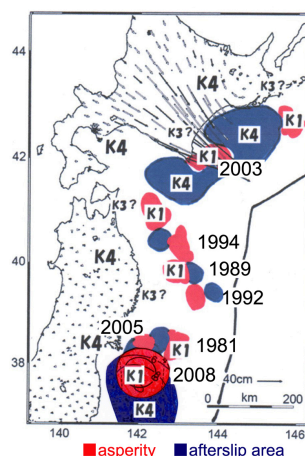
(K2)  $a-b < 0$ ,  $l$  between (K1) and (K3) : stability transition mode, where silent earthquakes recur in the last stage of the seismic cycle.

(K3)  $a-b < 0$ ,  $l$  large : substable sliding mode.

(K4)  $a-b > 0$  : stable sliding mode, where stale sliding is dominant throughout a seismic cycle. When the dynamic rupture occurs in the adjacent asperity, this area act as barrier and if the rupture invade, the rupture is turned into afterslip.

Thus, I would like to propose a hypothesis that the afterslip areas associated with the 1992 Sanriku-oki and the 2008 Fukushima-oki earthquakes have acted as barriers to expansion of major rupture of the 2011 Tohoku earthquake. I also would like to re-emphasize importance of the frictional law of fault slip to understand earthquake physics.

Keywords: 2011 Tohoku earthquake, asperity, afterslip, barrier, friction law



## Active faults and large earthquakes around the Japan Trench

WATANABE, Mitsuhsisa<sup>1\*</sup>, NAKATA, Takashi<sup>2</sup>, SUZUKI, Yasuhiro<sup>3</sup>, GOTO, Hideaki<sup>2</sup>, KUMAMOTO, Takashi<sup>4</sup>, TOKUYAMA, Hidekazu<sup>5</sup>, NISHIZAWA, Azusa<sup>6</sup>, KIDO, Yukari<sup>7</sup>, Shota Muroi<sup>4</sup>

<sup>1</sup>Toyo Univ., <sup>2</sup>Hiroshima Univ., <sup>3</sup>Nagoya Univ., <sup>4</sup>Okayama Univ., <sup>5</sup>Univ. of Tokyo, <sup>6</sup>Japan Coast Guard, <sup>7</sup>JAMSTEC

We investigated feature of active structures around Japan trench based on 3D anaglyph images. There is an extensive reverse fault ca. 500-km long with long anticlinal bulge on its hanging wall in the landward slope of the trench. The accumulated vertical displacement is over 1,000-3,000 meters, which indicates that the active fault has originated very large earthquakes. The 2011 off the Pacific of Tohoku Earthquake (M9.0) was the same as the previous characteristic earthquakes of the active fault. Other submarine active faults are also recognized close to the hypocentral regions of historical large earthquakes. It is essential to examine submarine active faults in order to make an accurate estimate of future large earthquake. According to the relationship between historical earthquakes and submarine active faults, there are two large seismic gaps along Japan trench. We need prepare for large earthquakes that may occur in these regions.

Keywords: submarine active fault, large historical earthquake, tsunami, seismic gap, Japan Trench



## Preliminary report on paleotsunami deposits survey in Higashidori Village, Aomori Prefecture, northern Japan

TANIGAWA, Koichiro<sup>1\*</sup>, SAWAI, YUKI<sup>1</sup>, SHISHIKURA, Masanobu<sup>1</sup>, NAMEGAYA, Yuichi<sup>1</sup>

<sup>1</sup>Geological Survey of Japan

The rupture area of the 2011 off the Pacific coast of Tohoku Earthquake covers approximately 400 km in length along Japan Trench, and this earthquake raised concerns about future large earthquakes in the north (offshore northern Sanriku) and south (offshore Boso) of the rupture area by changes in balance of stress (Simons et al., 2011). However, there are few historical and geological records to evaluate long-term earthquake history around north and south of Japan Trench. From this perspective, we began geological study of paleotsunami in the Shimokita Peninsula, facing around the boundary between Kuril Trench and Japan Trench.

We found at least three wide-spread sand sheets beneath a narrow valley in Higashidori. The sand sheets are medium to coarse, quartz-rich, and interbedded with clay, peaty clay, or peat. One of the sand sheets was found above a historical volcanic ash B-Tm, of which age shows 10th century. Radiocarbon ages from plant macrofossils just below the sand sheet range 1460-1650 AD and 1480-1650 AD. The other deeper sand sheets were found 200-240 cm and 250-300 cm in depth of the core, but we have not obtained ages yet.

### Reference cited;

Simons et al. 2011. The 2011 magnitude 9.0 Tohoku-Oki Earthquake: Mosaicking the megathrust from seconds to centuries. *Science* 332, 1421-1425, doi: 10.1126/science.1206731.

Keywords: tsunami deposit, Shimokita Peninsula, Japan Trench, Kuril Trench

## Reexamination of the tsunami trace of Hachijo Island in the 1605 Keicho earthquake

FURUMURA, Takashi<sup>1\*</sup>, IMAI, Kentaro<sup>3</sup>, MAEDA, Takuto<sup>1</sup>, HARADA, Tomoya<sup>2</sup>

<sup>1</sup>CIDIR/ERI Univ. Tokyo, <sup>2</sup>ERI UnlesTokyo, <sup>3</sup>DCRC Graduate School of Engineering, Tohoku Univ.

During the 1605 Keicho earthquake, large tsunami attacked to the large area from Boso Peninsula in Chiba to the Kagoshima bay in Kyushu. Since no strong ground motion was observed during the earthquake it is thought a tsunami earthquake occurred aking the Nankai trough subduction zone.

Because of the Japanese historical backdrop in the beginning of the 17th century, historical records of tsunami damage from this earthquake is very limited. In it, the fact that 57 persons were killed by tsunami in Hachijo Island is an important historical fact, which is based on description of "Hachijo Jikki". Hatori (1975) had pointed out a possibility that the tsunami of a maximum of 10 to 20 m attacked the Hachijyo Island. Since then his opinion has had big influence on the tsunami disaster prevention for Tokai to Kanto area expected for future Nankai Trough earthquake.

The tsunami simulation which assumed the tsunami model for Tokai-type earthquake with fault rupture run from off Tokaido to Suruga bay show the tsunami height at Hachijo Island is about 5-6 m at most. Thus, it is very difficult to reproduce tsunami over 10 m without assuming special phenomenon for the earthquake source model. Actually, Aida (1981)claimed that the extreme tsunami source model which assume that the fault rupture run along the Sagami trough off Boso and Izu Mariana Trench is needed in addition to the ordinary Tokai earthquake model along the Nankai Trough off Tokaido, in order to explain this high tsunami. On the other hand, Yamamoto (1995) scrutinizes the record tradition of the tsunami described in the account of Hachijo Jikki, a map colony position of those days, and the geographical feature of the Island and concluded that the tsunami height of Hachijo Island in the Keicho earthquake was not having reached 10 m. Watanabe (1998) adopted that the height of tsunami during the earthquake is less than 7-8m.

We re-scrutinized the description of the height of tsunami in the Hachijyo Jikki, and conducted a field survey on 25-27 September, 2011 for reexamination of the Keityo earthquake tsunami. We concluded that the height of tsunami in Hachijyo Island was at most 7-8 m and it did not exceed 10m.

## Possibility of a hyper earthquake in Southwestern Japan

FURUMOTO, Muneyoshi<sup>1\*</sup>

<sup>1</sup>Nagoya University, Graduate School of Environmental Studies

Recently it has been recognized that the subduction zone along the Suruga and the Nankai troughs in SW Japan has a potential for an M9-class earthquake, which will be much larger than the 1707 Hiei earthquake. In this assumption, while the source area comprises many fault segments including a deeper part of the subduction zone, the maximum dislocation on the fault is postulated to be smaller than that of the 2011 Tohoku earthquake (M=9.0). However, there is a possibility that the largest earthquakes along the subduction zone may involve a dislocation as large as the Tohoku event, several tens of meters. In order to investigate such a possibility we should invoke data from geological and/or archeological fields, since historical records on earthquakes for the last 1000 years must be insufficient. Based on data of coastal terraces formed in the last 6000 years, I report it is likely that huge events took place repeatedly in the relevant region. Three or four remarkable terraces have been formed at the coasts on the peninsulas, Omaezaki, Shiono-Misaki, and Muroto-Misaki, along the subduction zone (Fujiwara et al., 2004; Shishikura., 2008; Maemoku, 2001). Since the vertical displacements between the terraces are large and the average interval is longer than that proposed for the Hiei-type events, the terrace forming events should be different from the Hiei-type earthquake. The reported ages of the terraces at Shiono-Misaki and Muroto-Misaki are similar to each other. They were formed 4500-4800 years ago, 2700-3000 years ago, about 1800 years ago, and several hundreds years ago. Although the ages of the terraces at Omaezaki are not given accurately, the number of the terraces agrees with those at the other two sites. It is likely that the events forming the terraces are not local phenomena but regionally wide ones. Moreover, there are similar terraces in a wide area in SW Japan. These crustal movements suggest a possibility that hyper earthquakes with large fault areas and dislocations have repeated in SW Japan as well as the Tohoku region of Japan.

Keywords: subduction zone, terrace

## Two historical tsunami deposits recognized in the core sediments along the Hamana River on the Enshu-nada coast, Central

SATO, Yoshiki<sup>1\*</sup>, FUJIWARA, Osamu<sup>2</sup>, ONO, Eisuke<sup>3</sup>, Toshifumi Yata<sup>4</sup>, UIMITSU, Masatomo<sup>5</sup>

<sup>1</sup>Kyushu Univ., JSPS Research Fellow, <sup>2</sup>AFERC, AIST, <sup>3</sup>Faculty of Education, Niigata Univ., <sup>4</sup>Faculty of Humanities, Niigata Univ., <sup>5</sup>Faculty of Letters, Nara Univ.

The Lake Hamana is located along the Nankai trough, where interplate earthquakes have often occurred repeatedly (Shizuoka Pref., 1996). We analyzed diatom fossil assemblages of samples taken from the Arai No. 1 core (Fujiwara *et al.*, 2010). As the result, two historical tsunami deposits are recognized. Radiocarbon ages indicate that the lower deposited at the AD1498 Meio earthquake and the upper at the AD1707 Hoei earthquake or AD1854 Ansei earthquake.

The Arai No.1 core was excavated in a small flood plain between the Peistocene marine terraces and the Holocene sand dunes in the southern part of the Lake Hamana. This plain is consisted of an abandoned channel of the former Hamana river and back-marshes. According to the core stratigraphy (Fujiwara *et al.*, 2010), this core sediment is composed of channel deposit of the former-Hamana river (lower 3.45 m of the core) and a swamp deposit (upper 2.9 m of the core). The upper 0.9 m part of the channel deposit is sandy sediments with many molluscan fossils. Radiocarbon ages taken from this lowland suggest that the upper part deposited around the Meio earthquake (Fujiwara *et al.*, 2010). We performed diatom analyses about the 33 subsamples taken from the core in interval of 2-41 cm. Subsamples were treated based on Kosugi(1993).

Diatom assemblages enabled to be classified the core sediments into 5 diatom zones. The Zone I (3.54, 3.70 and 3.34 ? 3.52 m depth) is characterized by dominance of brackish-marine species such as *Cocconeis scutellum* and *Achnanthes hauckiana*. In the Zone II (2.53 to 3.32 m depth), however, *C.scutellum* and *A. hauckiana* decrease less than 10 % respectively, and *Staurosira construens* increases up to 20-50% with other fresh water species such as *Synedra tabulate* and *Cocconeis placentula*. The Zone III (1.36 - 2.40 m depth) and the Zone IV (1.16 - 0.96 m depth) is resemble each other with abundance of *S. construens* and *Pinnularia* spp. The Zone V (1.27 - 1.33 m depth) is corresponding to the muddy layer between the swamp deposits (1.25-1.33 m depth) and characterized by the spike of marine species of *Thalassiosira* sp. occupying approximately 10-40 %. This muddy layer is recognized successively in horizontal direction in eastern part of the lowland.

The Zone II shows obvious increasing of fresh-marine diatom species instead of brackish-marine species. This indicates that environmental change from river mouth to fresh-brackish marsh or pond. Stratigraphy and radiocarbon ages show that this environmental change occurred rapidly after the Meio earthquake. On the other hand, the dominance of outerbay diatom species in the Zone V indicates that marine water flowed into the fresh water marsh from the Pacific Ocean due to a tsunami current. Radiocarbon ages around the core indicate that the zone V was formed at the AD1707 Hoei earthquake or AD1854 Ansei earthquake. The Zone V shows similar core faces to the fore-end of the tsunami deposit of the 2011 Tohoku earthquake (Fujiwara *et al.*, 2011). The upper tsunami deposit including the Zone V has 8 cm thickness at least, therefore it suggests that inundation limit of the tsunami flows was further inland than the Arai No.1 core site.

### Reference

Fujiwara *et al* 2010. Geomorphic impact by the1498 Meio earthquake along the Hamana River on the Enshu-nada coast, central Japan: Evidence from the cored sediments. Historical Earthquakes (Rekishi Jishin), 25, 29-38.

Fujiwara *et al* 2011. Sedimentary features of the 2011 Tohoku earthquake tsunami deposit, on the Hasunuma coast (Central part of the Kujukuri coast), east Japan., Annual Report on Active Fault and Paleoeearthquake Reaserches, 11, 1-11.

Kosugi, M., 1993. Diatom. In A Handbook of Quaternary Research, vol. 2 (Japan Association of Quaternary Reaserch, Eds.), 245-252. Tokyo. University of Tokyo Press. (in Japanese).

Shizuoka Prefecture., 1996. History of Shizuoka Prefecture, separated volume no.2, history of natural disasters. Shizuoka Prefecture, Shizuoka, 808 pp. (in Japanese).

Keywords: Lake Hamana, Tsunami deposit, Meio earthquake, Diatom fossil assemblage, Nankai trough

## Petrophysical properties of fossilized seismogenic megasplay fault

HAMAHASHI, Mari<sup>1\*</sup>, SAITO, Saneatsu<sup>2</sup>, KIMURA, Gaku<sup>1</sup>, YAMAGUCHI, Asuka<sup>1</sup>, FUKUCHI, Rina<sup>3</sup>, KAMEDA, Jun<sup>1</sup>, HAMADA, Yohei<sup>1</sup>, FUJIMOTO, Koichiro<sup>3</sup>, HASHIMOTO, Yoshitaka<sup>4</sup>, HINA, Shoko<sup>1</sup>, EIDA, Mio<sup>4</sup>, KITAMURA, Yujin<sup>2</sup>, MIZUOCHI, Yukihiko<sup>5</sup>

<sup>1</sup>Department of Earth and Planetary Science, the University of Tokyo, <sup>2</sup>Institute for Research on Earth Evolution, Japan Agency for Marine-Earth Science and Technology, <sup>3</sup>Faculty of Education, Tokyo Gakugei University, <sup>4</sup>Department of Natural Environmental Science, Faculty of Science, Kochi University, <sup>5</sup>Sumitomo Resources Exploration & Development, Co., Ltd.

To understand the evolution and fault mechanism of subduction zone megasplay fault branching from plate boundary, Nobeoka Thrust Drilling Project (NOBELL) was carried out in 2011. Nobeoka Thrust is known to be a fossilized megasplay fault (out-of-sequence thrust) in ancient accretionary complex, located onland in Kyushu, Japan. In this project, coring and wireline logging were conducted down to 255m in total depth across the Nobeoka Thrust. Continuous logs of resistivity, density neutron porosity, natural gamma ray, and optical/sonic images were successfully acquired along the borehole wall.

In this study, we focus on the interval of 20-60m, including the main fault core (at 41m), and compare the physical properties among hanging wall, footwall, and fault core, correlating logging datasets and core description. Structure of hanging wall is characterized by phyllite and relatively stable foliation. Stronger deformation and boudinage can be seen from ~38m toward fault core. Random fabric cataclasite characterizes fault core, while cataclasite / foliated cataclasite are spread throughout footwall.

Footwall presents higher values of neutron porosity (4.6-10.5%) compared to hanging wall (2.3-8.7%), while porosity is lowest (3.2-10.2%) around fault core. Resistivity is higher at hanging wall (SN: 138-622 ohm-m), followed by drop near fault core (151-203 ohm-m) and stably lower footwall (163-323 ohm-m). P-wave velocity is highly fluctuated and slightly higher at hanging wall and higher values at fault core (3.3-5.0m/s) and values are stable at footwall (3.8-4.6m/s). Local decreases in natural gamma ray (91.9-134 API) and spontaneous potential (39.4-57mV) are characteristic around fault core, while values are nearly constant at hanging wall (81-158 API, 18.7-64.2mV) and footwall (91.1-152 API, 53.3-59.7mV). Density log is fluctuated and does not show significant changes throughout depth (2.4-2.9g/cc).

Crossplots of these logging data are useful to examine relationship between the logs and extract different responses with depth. A resistivity-porosity plot clearly illustrates that the fault core, hanging wall, and footwall show different trend. We also apply empirical formulas (such as Archie's formula and Wyllie's formula) to evaluate relationship between physical properties and internal structure and characterize hydrological properties. Permeability derived from porosity and resistivity show highest values around fault core, despite the lowest porosity value at the interval. These results provide important suggestions to understand structural and hydrological properties associated with fault activities and to connect modern and ancient seismogenic megasplay faults.

## Illite crystallinity of the borehole samples penetrating the Nobeoka thrust, Miyazaki prefecture, SW Japan

FUKUCHI, Rina<sup>1\*</sup>, FUJIMOTO, Koichiro<sup>1</sup>, HAMAHASHI, Mari<sup>2</sup>, YAMAGUCHI, Asuka<sup>2</sup>, KIMURA, Gaku<sup>2</sup>, KAMEDA, Jun<sup>2</sup>, HAMADA, Yohei<sup>2</sup>, HASHIMOTO, Yoshitaka<sup>3</sup>, HINA, Shoko<sup>2</sup>, EIDA, Mio<sup>3</sup>, Yujin Kitamura<sup>4</sup>, Saneatsu Saito<sup>4</sup>, Yukihiro Mizuochi<sup>5</sup>, Kazunori Hase<sup>5</sup>, Takayuki Akashi<sup>5</sup>

<sup>1</sup>Tokyo Gakugei University, <sup>2</sup>The University of Tokyo, <sup>3</sup>Kochi University, <sup>4</sup>JAMSTEC, <sup>5</sup>Sumiko Resource Exploration & Development, Co.,Ltd.

A borehole penetrating the Nobeoka thrust was drilled at Nobeoka city, SW Japan as analogue of NanTroSEIZE project. The Nobeoka thrust is a fossilized OOST in the Shimanto belts, Cretaceous and Paleogene accretionary complex in SW Japan. Total drilling length was 255m and continuous core samples were recovered. The borehole runs through the Nobeoka thrust at the depth of 41.7m. The hangingwall is Kitagawa group mainly consist of phyllite and the footwall side is melange of Hyuga group (Kondo *et al.*, 2005).

In the present study, we present preliminary results of X-ray diffraction analysis of the fragmented core samples. Constituent minerals are mainly quartz, plagioclase, illite, chlorite and calcite. The mineral assemblages are almost the same from the top to the bottom. We determined illite crystallinity (illite crystallinity, IC), one of the indicator of paleotemperature, using oriented samples.

IC values in the hangingwall range from 0.163 to 0.185°, those in the main thrust zone range from 0.678 to 0.701°, and those in the footwall ranges from 0.369 to 0.550°. The IC values show clear difference among the hangingwall, the main thrust zone and footwall. The paleotemperatures, calculated after the conversion formula (Mukoyoshi *et al.*, 2007), are 315-319°C in the hangingwall, 209-213°C in the thrust zone and , 240-277°C in the footwall. Vitrinite reflectance analyses indicate that the maximum temperatures of the hanging wall and footwall are approximately 320and 250°C, respectively (Kondo *et al.*, 2005), which agree to our results.

On the other hand, the samples in the main thrust zone indicate a larger IC values and lower paleotemperatures. The later faulting and alteration under lower temperture probably affected only on the main thrust zone, though the mineral assemblages do not show remarkable change.

Keywords: Fault, Borehole core, Accretionary Complex



## Stress analysis on various deformation features in on-land accretionary complexes: Shimanto Belt, Shikoku, SW Japan

EIDA, Mio<sup>1\*</sup>, HASHIMOTO, Yoshitaka<sup>1</sup>

<sup>1</sup>Kochi University

At an accretionary subduction zone, sediments are deformed by underthrusting, accretion, and earthquake. Corresponding deformation features are identified in on-land accretionary complexes such as tectonic melanges, shear veins, underplating faults, out of sequence thrusts, and localized faults with pseudotachylyte. Those deformation features are formed under different stresses and stages. Furthermore, those changes in stress and stages of deformation reflect change in physical properties and fluid pressures along subduction interface, which is strongly related to architecture and strength of accretionary wedges and seismic behavior. The purpose of this study is to understand the time-spatio changes in deformations and stress along subduction interface from on-land accretionary complexes.

The study areas are Yokonami melange (Cretaceous) and Mugi melange (Cretaceous and Paleogene). Both are in Shimanto Belt, Shikoku, Southwest Japan. They are composed mainly of sandstone blocks and black shale matrix with minor basalt, chert and tuff. The localized slip zones, the Goshikino-hama fault for Yokonami melange and the Minami-awa fault for Mugi melange, are identified at the northern boundary of the melange zones. Shear veins are well developed both in the melange zones. Slicken lines and slicken steps are well preserved on the shear vein surfaces. In the Mugi melange, underplating faults at the bottom of the oceanic basements are well exposed. Fluidization was reported along the underplating fault.

For stress analysis, we used Multiple inverse method (MIM, Yamaji, 2000) and Hough inversion method (HIM, Yamaji, 2006). Examined deformation features are 1) shear veins in Yokonami melange, 2) faults at the Goshikino-hama fault, 3) shear veins in Mugi melange, and 4) underplating fault in Mugi melange. Comparing between MIM and HIM, we found that the MIM provided a better result on the basis of misfit analysis. Therefore, we use stress from MIM. Further, we use one stress for each deformation feature with the smallest misfit in the following discussion.

To compare the results of stress, the stress orientations are reconstructed by rotations of fault planes to be horizontal because the averaged orientation of foliation is varied between deformation features and those fault planes would be horizontal at the time of deformation. The obtained stresses are as following. 1) A low angle N-S compression with 0.32 of stress ratio for shear veins in Yokonami melange, 2) a low angle NE-SW compression with 0.22 of stress ratio for the Goshikino-hama fault, 3) a low angle NNE-SSW compression with 0.05 of stress ratio for shear veins in Mugi melange, and 4) a low angle E-W compression with 0.45 of stress ratio for underplating fault, where stress ratio is defined as  $(\sigma_2 - \sigma_3)/(\sigma_1 - \sigma_3)$ . The orientations of stresses for 1), 2) and 3) are similar to each other. On the other hand, the stress orientations and stress ratio for 4) is completely different from others.

Effective frictional coefficient ( $M'$ ) was also examined by the lowest ratio between normal and shear stresses on fault planes as suggested by Angelier (1989).  $M'$  are related to frictional coefficient  $M$  and fluid pressure ratio  $\lambda$  as following equation.

$$M' = M(1 - \lambda)$$

Obtained effective frictional coefficients for each deformation feature are 1) 0.11-0.48, 2) 0.49-0.79, 3) 0.14-0.35, and 4) 0.05-0.23.  $M'$  for the Goshikino-hama fault is relatively high, indicating decrease of fluid pressure at the time of fault activity. Others have relatively low  $M'$ . Shear veins have a much of precipitated quartz and calcite. Those minerals suggests that large amount of fluid are existed for the deformation. The lower  $M'$  for underplated fault can be explained by the fluidization along the fault that was reported by previous study.

Keywords: paleostress, subduction zone, accretionary complex, melange, underplating fault, effective frictional coefficient



## Development of geo- and fault-thermometer using a raman spectroscopy tecqbuque on carbonaceous material

HIDEKI, Mukoyoshi<sup>1\*</sup>, KITAMURA, Manami<sup>2</sup>, HIROSE, Takehiro<sup>3</sup>, YAMAMOTO, Yuzuru<sup>4</sup>, SAKAGUCHI, Arito<sup>4</sup>

<sup>1</sup>Marine Works Japan Ltd., <sup>2</sup>Hiroshima University, <sup>3</sup>JAMSTEC Kochi, <sup>4</sup>JAMSTEC

In order to develop geothermometer of low-grade metamorphic rocks, we examined Raman spectrum of poorly-ordered carbonaceous materials (CM) with different metamorphic temperatures. The CM samples used in this study were collected from the Miocene Hota complex (50°C) (Yamamoto et al., 2005), the Cretaceous Shimanto complex (150°C and 230°C) (Mukoyoshi et al., 2006) and the Jurassic Ashio complex (300°C) and measured the Raman spectra. In addition, the CM is also matured by frictional heating of a fault even during short-periods coseismic sliding (several seconds' process) (e.g., O'Hara et al 2006). Such maturation of CM can be used for a fault-thermometer to estimate frictional heat along a fault during an earthquake. Thus, we performed laboratory friction experiments on CM to determine how the Raman spectra of the CM change with frictional heat. The experiments were conducted simulated gouge (a mixture of 90 wt% quartz and 10 wt% vitrinite) at slip velocities of 0.0013-1.3 m/s, normal stress of 1.0 MPa and displacement of 15 m under anoxic, nitrogen atmosphere, while measuring temperature in the gouge zone by thermocouples.

Here, we present our preliminary attempt for developing a geothermometer using Raman spectra of CM. On poorly-ordered carbonaceous materials, first-order Raman spectrum often decomposed into four peaks of a Raman shift (G peak at about 1580cm<sup>-1</sup>, D1 peak at about 1350cm<sup>-1</sup>, D2 peak at about 1620cm<sup>-1</sup>, D3 peak at about 1500cm<sup>-1</sup>) (e.g., Bayssac et al., 2002; Aoya et al., 2010). In our amorphous CM (coal) samples we recognized other three peaks on the D1 peak around 1150 cm<sup>-1</sup>, 1220 cm<sup>-1</sup> and 1450 cm<sup>-1</sup>. The first-order Raman spectra of our coal samples, in particular low-temperature samples, are hard to fit with decomposed four peaks using the LabSpec program due to the influence of faint shoulders on D1. However, the Raman spectra can be fit well when we used the above seven peaks. In this study, we define an area ratio of D1/[decomposed seven peaks] as R6. The correlation between R6 and T is given by

$$T (^{\circ}\text{C}) = 10.9 * \exp(11.9 * R6) \quad (R^2 = 0.99)$$

These correlations can be used for a potential geothermometer for low-grade metamorphosed sediments, in the temperature range of 50-300°C. We will present a potential fault thermometer using Raman spectra of CM in the meeting.

Keywords: raman spectroscopy, vitrinite reflectance, carbonaceous material, geothermometry, frictional heat, fault rock

## Sensitivity analyses of slip parameter estimation to hydrological and thermal properties

HAMADA, Yohei<sup>1\*</sup>, SAKAGUCHI, Arito<sup>2</sup>, TANIKAWA, Wataru<sup>1</sup>, YAMAGUCHI, Asuka<sup>1</sup>, KAMEDA, Jun<sup>1</sup>, KIMURA, Gaku<sup>1</sup>

<sup>1</sup>Department of Earth and Planetary Science, The University of Tokyo, <sup>2</sup>Japan Agency for Marine-Earth Science and Technology, <sup>3</sup>Japan Agency for Marine-Earth Science and Technology, Kochi I

Sensitivity analyses of slip parameter estimation to hydrological and thermal properties

Yohei Hamada<sup>1,\*</sup>, Arito Sakaguchi<sup>2</sup>, Wataru Tanikawa<sup>3</sup>, Asuka Yamaguchi<sup>1</sup>, Jun Kameda<sup>1</sup>, Gaku Kimura<sup>1</sup>

<sup>1</sup>Department of Earth and Planetary Science, University of Tokyo, 7-3-1 Hongo, Bunkyo-ku, Tokyo 113-0033, Japan

<sup>2</sup>Institute for Research on Earth Evolution, Japan Agency for Marine-Earth Science and Technology, 3173-25 Showa-machi, Kanazawa-ku, Yokohama 236-0001, Japan

<sup>3</sup>Kochi institute for Core Sample Research, Japan Agency for Marine-Earth Science and Technology, 200 Monobe Otsu, Nankoku-city, Kochi, Japan

\* yhamada@eps.s.u-tokyo.ac.jp

### Abstract

Enormous earthquakes repeatedly occur in subduction zones, and the slips along megathrusts, in particular those propagating to the toe of the accretionary prism, generate ruinous tsunamis. Although quantitative evaluation of slip parameters (i.e., slip velocity, rise time and slip distance) of past slip events for the shallow, tsunamigenic part of a fault is a critical component of characterizing such earthquakes, it is very difficult to constrain these parameters. Here we quantify these parameters for slip events that occurred along the shallow part of a megasplay fault and a plate boundary decollement in the Nankai Trough, off Japan. We applied a kinetic approach to profiles of vitrinite reflectance data obtained from Integrated Ocean Drilling Program (IODP) cores that intersected the slip planes of the two thrusts, and identified extremely slow and long-term slips in the megasplay fault and the frontal decollement.

The chemical kinetic method is useful to evaluate fault temperature and slip parameters. This has been introduced into various natural faults, however, this contains uncertainty due to its sensitivity to temperature which is dependent on various natural properties complicatedly. Therefore, we also discussed the effect of temperature dependence of thermal property or dynamic weakening mechanism for temperature calculation. We assessed the sensitivity of the calculation results to the measured thermal property and dynamic weakening effect caused by thermal pressurization.

Keywords: fault material, slip parameter, parameter sensitivity

## Relationship between compressional-wave velocity and porosity of sediments along subduction plate interface

YAMAGUCHI, Mika<sup>1\*</sup>, Yoshitaka Hashimoto<sup>1</sup>

<sup>1</sup>Kochi University

Evolution of physical properties of sediments along subduction interface has an effect on wedge strength, wedge geometry, dewatering and dehydration processes, and seismic behavior. Sediments have initially more than 70% of porosity prior to subduction. Through underthrusting and accretion, porosity of sediments decreases by compaction and cementation to be lithified sediments. The purpose of this study is to understand evolution of physical properties from a state before subduction to a state within a wedge using a relationship between compressional-wave velocity and porosity.

In this study, we obtained new data for sediments from a reference site in IODP NanTroSEIZE, Expedition 333, sites in Expeditions 315 and 316. In addition to that, we have compiled velocity-porosity relationships obtained by previous studies from NanTroSEIZE (off Kumano) (Hashimoto et al., 2010, 2011, Raimbourg et al., 2011), ODP Leg 190 (off Shikoku) (Hoffman and Tobin, 2004) and ODP Leg 170 (off Costa Rica) (Gettemy and Tobin, 2003).

Locations of sites are as following: For off Kumano, Site C0011 in Expedition 333 is in reference site (prior to subduction), Site C0006 is located at toe of accretionary prism, C0004 is located on a Megaseplay fault, Site C0001 is located at landward of C0004 and ocean-ward of Kumano basin, and C0002 is located in the Kumano basin above the seismogenic zone. For off Shikoku, Site 1173 and Site 1174 are located in reference sites, off Muroto and Off Ashizuri, respectively. For off Costa Rica, Site 1039 is located 1.5km of ocean-ward of deformation front (reference site), Site 1043 and Site 1040 are located in 0.6km and 1.7km landward from deformation front, respectively.

Velocity measurement procedure in this study to obtain new data is as following: In the velocity measurements, two pumps (Teledyne ISCO 1000D syringe pump) were used to control pore fluid pressure and confining pressure. The pore pressure of 1000kPa was kept under drained conditions. Confining (effective) pressure was increased stepwise in the measurements. Velocity measurements were conducted under isotropic pressure conditions. Confining pressure was pressurized in tens seconds and kept for more than 8 hours for next step to obtain equilibrium conditions between effective pressure and sediments strain. About 8 steps were conducted for each sample. A in situ effective pressure was approximated for each sample from the accumulation of the bulk density of sediments and hydrostatic pore fluid pressures at the depth of recovery. The maximum effective pressure for each test was up to about 2.5 times of in situ effective pressure. Lead zirconate titanate (PZT) shear wave transducers (500kHz) were used in a source-receiver pair to measure wave speed. PZT in a shear orientation generates a weak compressional mode in addition to its primary shear mode.

Porosity and P-wave velocity ranges about 27 ? 65% and 1.5 ? 2.6 km/s in this study. The P-wave velocity from Raimbourg (2011) is relatively about 1.0 km/s higher at corresponding porosity comparing with that from Hoffuman and Tobin (2004) and Hashimoto et al., (2011).

Sediments were classified into two, simply compacted sediments (reference site and slope sediments) and wedge sediments. Different trend in Vp-porosity relationships were observed for the classified sediments. For compacted sediments, Vp-porosity relationships are along the global empirical relationships (Erickson and Jarrard 1988) and within the area between normal and highly compaction curves. On the other hand, some of Vp-porosity relationships for wedge sediments represent trends with higher velocity at a porosity. Such trend was observed for wedge sediments from Site C0001, C0002 and even from Costa Rica. Those higher Vp trend in Vp-porosity relationship for wedge sediments can be explained by shear strain of sediments and or cementation.

Keywords: compressional-wave velocity, porosity, subduction plate boundary, accretionary complex

## X-ray CT imaging and hydrologic characterization of fractured core samples under stress

WATANABE, Noriaki<sup>1\*</sup>, ITO, Hisao<sup>2</sup>

<sup>1</sup>Tohoku University, <sup>2</sup>Japan Agency for Marine-Earth Science and Technology (JAMSTEC)

Analyzing fluid flow within naturally fractured samples under in-situ stress conditions is desirable. The present study first focuses on the feasibility of a precise 3D numerical modeling coupled with X-ray computed tomography (CT), which enables simple analysis of heterogeneous fracture flows within core samples, as well as the measurement of porosity and permeability. A numerical modeling was developed and applied to two fractured granite core samples having either an artificial single fracture or natural multiple fractures. With a linear relationship between the CT value and the fracture aperture, 3D distributions of the CT value for the samples were converted into fracture-aperture distributions in order to obtain fracture models for these samples. The numerical porosities reproduced the experimental porosities within factors of approximately 1.3 and 1.1 for the single fracture and the multiple fractures, respectively. Using the fracture models, a single-phase flow simulation was also performed. The numerically obtained permeabilities reproduced the experimental permeabilities within factors of 1.3 and 1.6 at for the single fracture and the multiple fractures, respectively. Consequently, a precise numerical modeling coupled with X-ray CT is essentially feasible. Furthermore, the development of preferential flow paths (i.e., channeling flow) was clearly demonstrated for multiple fractures, which is much more challenging to achieve by most other methods.

The method was then applied to two granite core samples having either a mated artificial or a mated natural fracture at confining pressures of 5 to 50 MPa. Numerical results were evaluated by a fracture porosity measurement and a solution displacement experiment using NaCl and NaI aqueous solutions. The numerical results coincided only qualitatively with the experimental results, primarily due to image noise from the aluminium liner of the core holder. Nevertheless, the numerical results revealed flow paths within the fractures and their changes with confining pressure, whereas the experimental results did not provide such results. Different stress-dependencies in the flow paths were observed between the two samples despite the similar stress-dependency in fracture porosity and permeability. The changes in total area of the flow paths with confining pressure coincided qualitatively with changes in breakthrough points in the solution displacement experiment. Although the data is limited, the results of the present study suggest the importance of analyzing fluid flows within naturally fractured core samples under in situ conditions in order to better understand the fracture flow characteristics in a specific field. X-ray CT-based numerical analysis is effective for addressing this concern.

Finally, a novel core holder with a carbon fiber reinforced polyetheretherketone (CFR PEEK) body has been proposed and developed. Medical CT scans for granite and sandstone samples containing a saw-cut fracture revealed that the core holder had no adverse influence on image quality due to the small X-ray attenuation. Moreover, with medical CT scans using the new core holder, a numerical analysis of single-phase flow was successfully completed on a fractured granite sample at confining pressures of 3-10 MPa, where real fracture porosities and permeabilities could be predicted within factors of 1.2-1.3 and 1.4-1.5, respectively. Although the maximum available confining pressure and sample size are currently limited due to the design, the novel core holder with the CFR PEEK body enables CT scans on fractured samples under confining pressure without image noise problem. Consequently, with the new core holder or a core holder having similar X-ray attenuation, the X-ray CT based numerical analysis can be successfully conducted on naturally fractured samples under confining pressure, which should contribute to better understanding of fluid flow characteristics in the crust.

Keywords: X-ray CT, hydrological characteristics, fracture, core sample, stress

## Seismic inversion of the incoming sedimentary sequence in the Nankai Trough off Kumano Basin, southwest Japan

NAITO, Kazuya<sup>1\*</sup>, PARK, Jin-Oh<sup>1</sup>

<sup>1</sup>Atmosphere and Ocean Research Institute, The University of Tokyo

Huge earthquakes have been repeated in the cycle of 100–150 years in the Nankai trough. The south western Japan have been struck terrible shakeups and tsunamis by these earthquakes. In these days the next emergence of the earthquake becomes one of the most serious issue in Japan. Therefore detailed description of geological structure is urgently needed to understand mechanism of the seismogenic zone of this area. Moreover, this area is getting attentions of scientists as the most surveyed subduction zone with accretionary prism in the world and recently becomes an important research target of IODP (Integrated Ocean Drilling Program). The seismic inversion technique is an inversion method to estimate physical parameters of layers on seismic profiles: in this method a seismic profile is modeled as convolution of measured physical properties with an estimated wavelet, and actual physical properties are estimated by the modeled seismic profile if the convolved profile shows good fitting with the observed one. We use 3D MCS (3D Multi-channel Seismic reflection survey) data which was acquired on KR06–02 research cruise in 2006, and measured physical properties of borehole logging and sediment cores by IODP Expedition 319 and 322 cruises in 2009. This study aims to challenge CLSI (Core–Logging–Seismic Integration) on the sediments layer of the Nankai trough.

Keywords: Nankai trough, Multi-channel Seismic reflection, sediments, seismic inversion

## Shallow structure and evolution of active faults with strike-slip in a forearc basin, eastern Nankai Trough

OJIMA, Takanori<sup>1\*</sup>, ASHI, Juichiro<sup>1</sup>, NAKAMURA, Yasuyuki<sup>2</sup>

<sup>1</sup>Atmosphere and Ocean Research Institute, the university of Tokyo, <sup>2</sup>Japan Agency for Marine-Earth Science and Technology

Accretionary prisms and forearc basins are developed in the Nankai Trough, SW Japan. Many active faults are recognized and classified into five fault systems in the eastern Nankai Trough. The Enshu Faults System, the most landward one, runs over 200 km along the northern edge of the Tokai, Enshu and Kumano forearc basins. Structural investigation of this area is important for earthquake disaster mitigation as well as understanding of oblique subduction tectonics. However, activity and distributions of faults has not been well clarified.

The Enshu Faults System has a general trend of ENE-WSW, on the basis of swath bathymetry and side-scan sonar imagery, and shows dextral strike slip inferred from displacement of the canyon axis across the landward-most fault. Seismic reflection profiles partly exhibit landward dipping faults. These observations suggest that this area is tectonically affected by oblique subduction of the Philippines Sea Plate.

We picked continuous reflectors and divided the formation into five units on the multichannel seismic profiles obtained by JOGMEC, and carefully studied thickness changes of the units across the faults, which reflect fault activities. Approximate positions of faults are estimated by discontinuities of seismic reflectors although fault planes are hardly recognized. Moreover, geometry of formations beneath the lineaments identified on the sidescan sonar imagery suggests existence of flower structures along fault zones. The formation thicknesses above the acoustic basement occasionally change across these fault zones. In most cases, the formation thickness seaward of the fault zones is thicker than that landward of them suggesting transpressive deformation. However, time and space distribution of unit thickness changes imply that fault displacements are not uniform along each fault zone. In order to know the recent fault activity, we carried out deep towed chirp subbottom profiler survey. In the base of the steep slope corresponding to the strong lineament, the shallow sedimentary sequence exhibits seaward divergent shape of reflectors. These depositional styles indicate recent activity of crustal movement by faulting although a fault plane is not recognized in the shallow sediment. In contrast, the dimmed seismic reflectors with tiny displacements were observed in the upper part of the slope. Shallow extension of the fault planes and existences of cold seep previously observed by a submersible survey suggest that these fault systems are still active at present.

Keywords: Oblique subduction, Strike-slip fault, Active fault, flexure



## Accumulation process of earthquake-induced turbid layer in the slope basin -An example from the Nankai Trough off Kuman-

SAWADA, Ritsuko<sup>1\*</sup>, ASHI, Juichiro<sup>1</sup>

<sup>1</sup>Aori, Univ. Tokyo

Earthquake shaking is one of triggers for submarine slope failures and causes sediment redeposition in the base of the slope. Sedimentary section of the slope basin in an accretionary prism continuously and well records past activity of earthquakes for a long term and with a high accuracy. Therefore, it is one of useful proxy to understand coseismic geological phenomenon. However, it is inferred that earthquake-induced turbid mud settles out so fast. In this study, because sedimentation processes on earthquake-induced sediment are not well illustrated so far, I am analyzing settling processes of earthquake-induced turbid mud in deep sea.

Muddy deposits in a deep-sea region generally show slow sedimentation rate. The velocity is several mm to several dozen mm per one thousand years. However, the observation by ROV "NSS" during KH-10-3 cruise (*R/V Hakuho-maru*) illustrated that thick turbid layers in the prism slope completely settled six years after the 2004 off Kii peninsula. Therefore, it is inferred that earthquake-induced turbid mud settles out during short period. Two turbid layers specifying different degrees of turbidity are composed of upper dilute suspension layer and bottom dense suspension layers. The measured water depth at the slope basin in 2010 shows high variation suggesting seafloor undulation. In contrast, the measured water depth in 2004 by NSS during KY04-11 cruise (*R/V Kaiyo*) was very constant. This observation indicates that the measured water depth corresponds to the upper boundary of a dense suspended layer as a pseudo-seafloor.

A chirp subbottom profiler (SBP) surveys were carried out during the KH-10-3 and KH-11-9 cruises. We successfully obtained high resolution structural images down to a maximum of about 30m. Sedimentary reflectors of the slope basin are mostly flat-lying and laterally coherent. Moreover, three transparent layers are developed at a depth shallower than about 10 meter below a seafloor. Observation of dense turbid layers after the 2004 earthquake and existence of distinct transparent layers in the slope basin suggest periodic accumulation of earthquake-induced turbid layer.

Keywords: turbid layer, redeposition, earthquake-induced sediments, sedimentary structure



## Closely-spaced heat flow measurements in the vicinity of the splay fault on the the Nankai accretionary prism

YAMANO, Makoto<sup>1\*</sup>, KAWADA, Yoshifumi<sup>1</sup>, HAMAMOTO, Hideki<sup>2</sup>, GOTO, Shusaku<sup>3</sup>

<sup>1</sup>Earthq. Res. Inst., Univ. Tokyo, <sup>2</sup>Center Environ. Sci. Saitama, <sup>3</sup>Geol. Surv. Japan, AIST

Heat flow measurements have been conducted in the Nankai Trough area southeast of the Kii Peninsula (off Kumano) for investigating the thermal structure of the target area of IODP seismogenic zone drilling (NanTroSEIZE). Combining the data obtained with ordinary heat-flow probe and long-term monitoring instruments with those estimated from gas hydrate BSRs, the overall pattern of heat flow distribution was delineated. Heat flow is around 100 mW/m<sup>2</sup> on the floor of the Nankai Trough and decreases landward to 40 to 60 mW/m<sup>2</sup> in the forearc basin (Kumano Trough), which should reflect the thermal structure of the seismogenic zone and the overriding plate. On the slope of the accretionary prism, however, highly scattered values (60 to 100 mW/m<sup>2</sup>) were obtained about 15 to 25 km landward of the deformation front, where the megasplay fault system approaches and intersects the surface. Possible causes of the scatter are: localized fluid flow along active faults, recent deformation near the surface including submarine landslides, bottom water temperature variation (BTV), and topographic disturbance.

To study the relation between the scattered heat flow and tectonic activities around the splay fault, we conducted closely-spaced heat flow measurements at two sites on the prism slope on KH-10-3 and KH-11-9 cruises of R/V Hakuho-maru in 2010 and 2011. One site is located around a prominent 400-m high scarp associated with a branch of the splay fault, At the foot of the scarp, biological communities have been found, indicating cold seepage activity along the fault. The observed heat flow is higher on the seaward side of the scarp and lower on the landward side. The highest values were measured at the foot of the scarp. The overall heat flow distribution across the scarp is attributable to the effect of bathymetric relief, whereas the local high at the foot of the scarp might arise from upward fluid flow along the fault. The other site is located around a U-shaped slump scar topography on the middle part of the prism slope and measurements were made along a line crossing the scar. The obtained data show no significant heat flow variation across the scar. It suggests that submarine landslide corresponding to the scar is not a very recent event.

We also conducted long-term temperature monitoring with pop-up type instruments and obtained bottom water temperature records for 15 months at two stations with water depths of 2550 and 3340 m. The record at the 2550-m station shows large BTV over 0.3 K, similar to the one previously obtained at about the same water depth. BTV with this amplitude has significant influence on temperature distribution in surface sediment. The BTV observed at the 3340-m station is much smaller, less than 0.1 K, and cannot cause appreciable variation in heat flow measured at the surface. Half of the existing scattered heat flow values were measured at sites shallower than 3000 m and may have been affected by BTV. We need to collect more long-term water temperature records at depths around 3000 m for evaluation of influence of BTV and for measurement of undisturbed heat flow.

Keywords: Nankai Trough, heat flow, accretionary prism, splay fault, cold seep, submarine landslide

## Back-ground seismicity within the Philippine Sea Plate off Shiono-misaki based on ocean-bottom seismographic observation

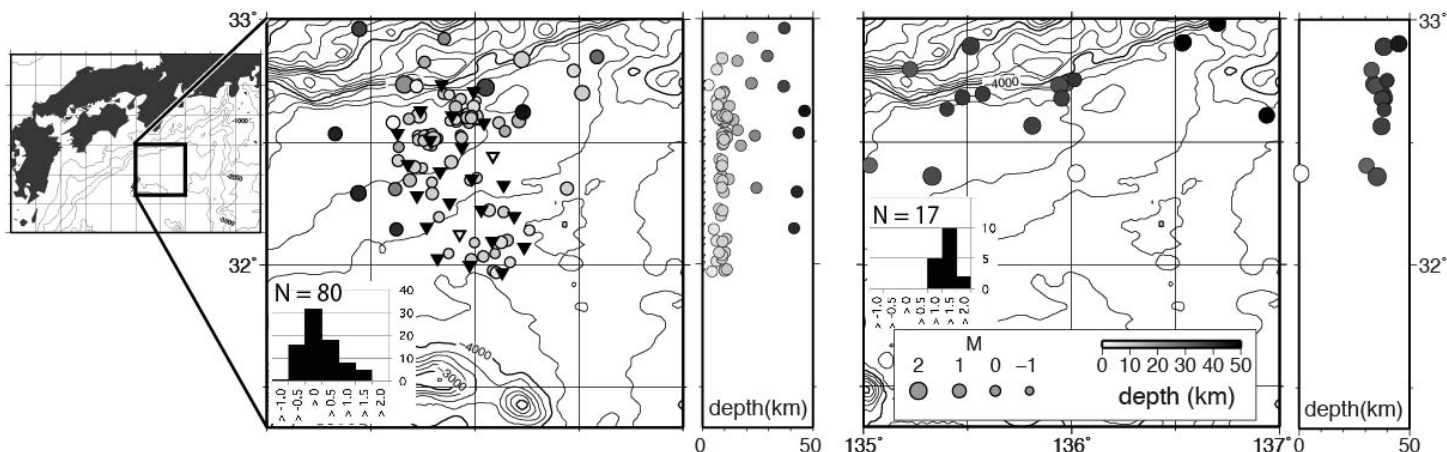
HIRATA, Kenji<sup>1\*</sup>, Hiroaki Tsushima<sup>1</sup>, Akira Yamazaki<sup>2</sup>, Hisatoshi Baba<sup>3</sup>, Hiroshi Sarukawa<sup>3</sup>, Akio Kobayashi<sup>1</sup>, Hiroshi Ueno<sup>1</sup>, Shigeki Aoki<sup>1</sup>, Yasuhiro Yoshida<sup>1</sup>, Akio Katsumata<sup>1</sup>, Kenji Maeda<sup>1</sup>, Takashi Yokota<sup>1</sup>

<sup>1</sup>Meteorological Reseach Institute, <sup>2</sup>Kakioka Magnetic Observatory, <sup>3</sup>Tokai University

From 2005 to 2008, we repeated short-term ocean-bottom seismic (OBS) observation four times to confirm ambient micro-seismicity at depths between about 10 km and 25 km beneath the axis of the Nankai Trough off Cape Shiono-misaki in Kii Peninsula, southwest Japan (Yamazaki et al., 2011, Tech. Rep. MRI). This micro-seismicity is poorly recorded by land seismic networks. Obana et al.(2005, JGR) distinguished them into two groups; shallow microearthquakes occurring within the oceanic crust of the incoming Philippine Sea Plate (PSP) (around 10 km in depth) and deep ones occurring in the uppermost mantle of PSP (about 15 km to 25 km in depth). They also reported that composite focal mechanisms of the shallow microearthquakes showed extensional stress in the direction nearly normal to the trough axis and those of the deep ones showed compressional stress in the direction normal to the trough axis, indicating "bending" of the incoming PHP. If so, how far south from the Nankai Trough axis the plate bending stress starts and how it develops?

To investigate this problem, we conducted OBS observations to the south from the trough axis between mid June 2009 and mid September 2009. The OBS network consisted of 24 short-term OBSs (4.5 Hz, 3-comp.) with a spacing of about 15 km (8 n.m.). We recovered 22 OBSs after a three-month long development. Deployment and recovery of the OBSs were done with R/V Ryofu-maru of JMA. After a linear correction of internal OBS time stamp, we picked arrival times of P-waves, S-waves and PS converted waves, which the picking of last phases is required for finding a set of initial station correction (i.e., sediment layer correction). Then we determined hypocenters assuming an appropriate one-dimensional velocity structure estimated based on a nearby seismic refraction experiment (Kodaira et al., 2000, Science). Next averaged differences between observed travel time and estimated travel times (O-C times) for each OBS were calculated. The averaged O-C times were then added to the previous station correction values, and the hypocenters were relocated. We repeated this procedure two times.

Figure shows preliminary hypocenters located in this study for the first 30 days of the observation period. Open circles and closed inverted triangles indicate hypocenters and OBSs, respectively. Hypocenters deeper than 30 km occur only outside the OBS network, indicating that their depths are not constrained. Within the OBS network, we find that the smallest earthquakes with magnitudes less than 1, which are defined as "ultra-microearthquakes(UMEs)", occur around 10 km in depth (upper panel of figure). JMA land-based seismic network does not detect the activity (lower panel). The OBS network was arbitrarily positioned and UMEs are probably a widespread feature of the seismicity in the incoming plate. So we propose that similar UMEs occur in wider area outside of the present OBS network. Among the two groups of microearthquakes reported by Obana et al., the deep microearthquake activity in the uppermost mantle within the present OBS network can be identified in the northern region of the OBS network (near the trough axis) but not in the southern region (toward the outer-rise). This suggests that microearthquakes in the uppermost mantle of PHP only occur near the trough axis and farther landward.



## Fine-scale Seismicity of the subducting PHS plate around the Kii Peninsula

AKUHARA, Takeshi<sup>1\*</sup>, MOCHIZUKI, Kimihiro<sup>1</sup>, NAKAHIGASHI, Kazuo<sup>1</sup>, YAMADA, Tomoaki<sup>1</sup>, SHINOHARA, Masanao<sup>1</sup>, SAKAI, Shin'ichi<sup>1</sup>, KANAZAWA, Toshihiko<sup>1</sup>, UEHIRA, Kenji<sup>2</sup>, SHIMIZU, Hiroshi<sup>2</sup>

<sup>1</sup>ERI, Univ. of Tokyo, <sup>2</sup>SEVO, Kyushu Univ.

### **Introduction**

In southwestern Japan, the Philippine Sea (PHS) plate subducts along the NNW direction beneath the Eurasian plate. This plate has been known for its complex shape, less seismic activity and occurrences of megathrust earthquakes. Although many seismological studies have been done, their resolutions at the ocean area are still poor, mainly because these studies are based on on-land observations. Mochizuki et al. (2010) investigated the seismicity around the Kii peninsula using ocean bottom seismometers (OBSs), and revealed stepwise changes of seismic characteristics along the Nankai trough. In this study, we do not only extend the study area of Mochizuki et al. (2010) using on-land observations, but we applied waveform cross correlation analysis to relocate hypocenters with better resolution. As a result, we obtained some linear alignment of earthquakes.

### **Data**

We deployed at most 27 long-term OBSs for repeating one-year observations around the Kii peninsula by changing sites among 32 locations from November, 2003 to November, 2007. In addition, we included arrival time data from 45 land stations during the same period.

### **Relocation and Tomography Method**

We first located events using P and S-wave first arrival times. During this process, we assumed station-specific 1-D velocity structures, and determined the station corrections simultaneously to compensate for systematic errors mainly originating from slow S-wave velocities in the sediment layers. We located 3931 events, which included microearthquakes that were not listed in the JMA catalog. Then, we applied a Double-Difference tomography method [Zhang and Thurber, 2003] to the above results and obtained relocated hypocenters and 3-D velocity structures for both P- and S-waves. Because of the limited seismic activity in this area, it is important to make full use of the present marine data set. Therefore, we applied non-linear grid search method [Lomax et al., 2009] to the events whose hypocenter was not stably determined through the above processes. This method searches hypocenters and origin times using 3-D grid velocity model so that the Equal Differential Time (EDT) likelihood function can be maximum. We obtained 1059 events by this grid search. Finally, we calculated waveform cross-correlation for measuring arrival time differences, and applied the Double-Difference tomography method again.

### **Results**

We obtained the seismic velocity structure of the subducting PHS and overriding Eurasian Plates and seismicity from around the Kii Peninsula to the Nankai Trough axis. The dip angle of subduction increases from west to east. The seismicity in the slab varies between the east and west. In the west, earthquakes occurred in shallow part of the slab mantle (30~35 km depth), while they did not occur in the east. We found some linear alignments of earthquakes in this western shallow mantle. These alignments are oriented in NNE-SSW. We also revealed a large alignment of intra-slab earthquakes just below the Nankai trough. It is oriented N-S and dipping southwards.

Keywords: PHS plate, seismicity, subduction, OBS, waveform cross-correlation, tomography

## Daily monitoring of shear wave velocity and anisotropic structure using the reflected wave extracted from BBOBS data

TONEGAWA, Takashi<sup>1\*</sup>, FUKAO, Yoshio<sup>1</sup>, NISHIDA, Kiwamu<sup>2</sup>, SUGIOKA, Hiroko<sup>1</sup>, ITO, Aki<sup>1</sup>

<sup>1</sup>JAMSTEC, <sup>2</sup>ERI, Univ. of Tokyo

Temporal variation at subsurface structure has been recently detected by using seismic interferometry. This would be achieved by extracting waves propagating between two stations, and measuring the temporal variation of the extracted wave. For example, with the extracted surface wave, Brenguier et al. (2008) found that a velocity reduction and its relaxation occurred at and after the 2004 Parkfield Earthquake. Nakata et al. (2011) detected velocity changes between two stations deployed in vertical array, which was caused by the 2011 Tohoku-oki Earthquake. Moreover, reflection profile underneath a seismic station can be obtained by auto-correlation function of seismic noise. Chujo et al. (2011) constructed the reflected P wave from auto-correlation function of seismic records observed at BBOBS, and detected a temporal velocity change due to the 2005 Miyagi-oki Earthquake. In this study, we try to extract the reflected S wave by using horizontal components of BBOBS data, and also investigate whether temporal variation of the shear wave velocity and its anisotropic structure occurs or not.

We used 2 BBOBS deployed on the accretionary prism at the Nankai trough. The time period of the observation is from 2008/8 to 2009/9. This period contains the time in which the very low frequency earthquakes (VLFs) are active.

We applied a bandpass filter of 1-3 Hz to two horizontal components. The amplitude of the records was disregarded by keeping one-bit signal. We then synthesized the waveform by rotating two horizontal components with a step of 5 degrees, and calculated auto-correlation functions (ACFs) with a time length of 600 sec. The ACFs stacked for 1 day were prepared for approximately 400 days. Note that the ACFs of the waveform for all directions allow us to extract the reflected S wave with different polarization directions.

Our results show that the S wave reflected at the bottom of the accretionary prism can be seen in the ACFs for all directions. Interestingly, the travel time of the reflected S wave is varied as a function of polarization directions, which is considered to be the effect of anisotropic structure between the station and seismic discontinuity. The velocity change between the fast and slow S wave is approximately 3-4 %. Moreover, such reflections can be constructed with 1 day stacking of noise, allowing us to daily monitor the S wave velocity and its anisotropic structure. However, no temporal variations could be found at or after the VLF activity on 2009/3. In the presentation, in addition to the above result, we will also report that the temporal variation of travel time of the reflected S wave due to the 2011 Tohoku-oki Earthquake is observed by using BBOBS data deployed in the outer-rise.

Keywords: seismic interferometry, monitoring, accretionary prism, anisotropy, shear wave velocity

## Slow slip events and large thrust earthquakes triggered by afterslip in the Hyuganada region

NAKATA, Ryoko<sup>1\*</sup>, HYODO, Mamoru<sup>1</sup>, HORI, Takane<sup>1</sup>

<sup>1</sup>JAMSTEC

Slow slip events were detected after the December 1996 earthquake in the deeper region of the postseismic slip area with a recurrence interval of approximately 2 years with the durations of 0.5-1 year [Yarai et al.]. Three slow slip events have been detected since 2005.

We proposed a model of numerical simulation for the coexistence of afterslip for ~M7 earthquake and slow slip events in the Hyuganada region of Japan with the 3D geometry of the Philippine Sea plate [Nakata et al., 2011, SSJ]. While coseismic events are reproduced by the slip law, recurrence of slow slip events are qualitatively reproduced by using the slowness law even in the velocity range of afterslips and slow slip events, in addition to characteristic slip distances larger than seismic source. In our simulation, afterslip triggered a slow slip event, which was unidentified in geodetic observation. After the triggered slow slip event, spontaneous slow slip events occurred in the same area. Furthermore, a large earthquake was triggered in the slow slip event area by postseismic slip.

In this study, we compare the spatial and temporal distributions of stress, strength, and slip velocity before a triggered slow slip event and an earthquake with a sampling interval of one day. As a result, the triggering of either a slow slip event or an earthquake through postseismic slip is determined by slight differences in stress and strength around the source.

### Acknowledgments

This work was partly supported by the project "Evaluation and disaster prevention research for the coming Tokai, Tonankai and Nankai earthquakes" of the Ministry of Education, Culture, Sports, Science and Technology of Japan. The Earth Simulator was used for all simulations.



## Progress of borehole seismo-geodetic observation above the rupture zone of the Tonankai earthquakes.

ARAKI, Eiichiro<sup>1\*</sup>, KITADA, Kazuya<sup>1</sup>, KIMURA, Toshinori<sup>1</sup>, KINOSHITA, Masataka<sup>2</sup>, KANEDA, Yoshiyuki<sup>1</sup>

<sup>1</sup>JAMSTEC DONET, <sup>2</sup>JAMSTEC IFREE

Sensitive seismic and geodetic sensors were installed in seafloor boreholes drilled near the rupture zone of the Tonankai earthquakes to construct high-quality seismo-geodetic observatories in the seafloor. Three or more borehole observatories are planned in the area and these observatories are planned to connect to dense ocean floor network for earthquakes and tsunamis (DONET) for realtime long-term seismo-geodetic observation in the rupture zone of the Tonankai earthquakes and off-shore side of the zone. The construction of the borehole observatories began in 2009 at IODP C10 site where we installed temporal pore-fluid pressure sensor. In December, 2010, we installed the first permanent seafloor borehole observatory in the area in IODP C2 site with borehole sensors such as volumetric strainmeter, tiltmeter, broadband and strong motion seismic sensors, pore-fluid pressure sensors, and thermometers. It was necessary to check performance of the installed borehole sensors in the C2 observatory before starting long-term observation. Originally an ROV cruise was planned in March, 2011, which was cancelled due to the earthquake in March 11, 2011. With some delay, we were still able to check the performance of all the borehole sensors through ROV visits in JAMSTEC R/V Natsushima cruises NT11-09 in July 2011 and NT12E01 in January 2012. All sensors were checked and these performed well in the seafloor borehole. The data from the borehole broadband seismometer in the C2 observatory showed the borehole is 10-20 dB quieter in some of seismic frequencies, suggesting good observation environment for seismo-geodetic observation is established in the borehole. Pore-fluid pressure sensors in the C2 observatory were checked at the time of installation and continued continuous observation since the installation. We have not still started continuous observation with other sensors but we plan to start long-term observation in near future and we are also preparing connection of the C2 observatory to the DONET cable in January 2013.

Keywords: borehole, seismic, geodecy, Tonankai earthquake

## Operation and Construction of Dense Oceanfloor Network System for Earthquakes and Tsunamis (DONET/DONET2)

KANEDA, Yoshiyuki<sup>1\*</sup>, Katsuyoshi Kawaguchi<sup>1</sup>, Eiichiro Araki<sup>1</sup>, Hiroyuki Matsumoto<sup>1</sup>, Takashi Yokobiki<sup>1</sup>, Shuhei Nishida<sup>1</sup>, Jin-Kyu Choi<sup>1</sup>, Masayuki Hoshino<sup>1</sup>, Masaru Nakano<sup>1</sup>, Takeshi Nakamura<sup>1</sup>, Keisuke Ariyoshi<sup>1</sup>, Narumi Takahashi<sup>1</sup>, Shin-ichiro Kamiya<sup>1</sup>, Toshitaka Baba<sup>1</sup>

<sup>1</sup>JAMSTEC

DONET (Dense Oceanfloor Network System for Earthquakes and Tsunamis) is a real time monitoring system conducting long-term and extremely precision observation in the seafloor. Broad-band seismograph, strong motion seismograph, hydrophone, differential pressure gauge, quartz pressure gauge, and precision thermometer, are installed in multiple seafloor observation points. They are connected with landing station by submarine cable so that observed data is acquired in real time. It was completed to establish all of the 20 observation point was planned as DONET1 in August 2011, and currently going well in operation of real-time observation in the sea depth of a range from 1,900m to 4,300m, in Kumano-nada off Kii Peninsula. The data is used in research and analysis that will contribute to the sophistication of an early earthquake and tsunami warnings and to understand the Nankai trough seismogenic zone via physical phenomena around the shallow plate boundary such as slow slip and low frequency events.

On the other hand, it is insufficient just maintenance of observation network in the Kumano-nada which is the source region of the Tonankai earthquake, to capture the process of a series from the Tonankai earthquake to the Nankai earthquake. Especially when the Tonankai earthquake occurred ahead of the Nankai earthquake, it is essential to extension of the observation network to the west for evaluation of the time lag between the Tonankai and the Nankai earthquakes. Accordingly in JAMSTEC, a subsequent project has started to construct a new earthquake and tsunami observation system from west off the Kii peninsula to off Muroto coastal area since 2010 (DONET2). DONET2 has 350km backbone cable length and 7 nodes and 30 observation points is a larger system than the current DONET, DONET2 of 10KV high voltage enable to deploy a wider observation network. Currently, we decided outline of the cable route of DONET2 and then bathymetric survey, the seafloor visual inspection are ongoing even as design of the landing stations.

We will introduce the operation of DONET and progress of DONET2.

Keywords: DONET, DONET2, real time monitoring system, Tsunami, Nankai trough, Nankai earthquake



## Investigation into source depth of mud volcano in the eastern Mediterranean: A case study of Medee-Hakuho Mud Volcano

KIOKA, Arata<sup>1\*</sup>, ASHI, Juichiro<sup>2</sup>, MURAOKA, Satoru<sup>2</sup>, SAKAGUCHI, Arito<sup>3</sup>, NAKAMURA, Yasuyuki<sup>3</sup>, SATO, Tokiyuki<sup>4</sup>, TOKUYAMA, Hidekazu<sup>2</sup>

<sup>1</sup>Dept. EPS, Univ. Tokyo, <sup>2</sup>AORI, Univ. Tokyo, <sup>3</sup>IFREE, Jamstec, <sup>4</sup>Engr. Resource Sci., Akita Univ.

Present-day geodynamic framework in the Eastern Mediterranean Sea and the surroundings is characterized by a complex pattern of active thick-skin crustal tectonics resulting from various plate and microplate interactions [e.g., McKenzie 1972]. Moreover, thick impermeable barrier of the Messinian evaporates exists below the entire Eastern Mediterranean foredeeps exceeding 3 km in thickness [e.g., Polonia et al. 2002]. These geological frameworks result in the Mediterranean Ridge (MedRidge) differing from other accretionary complexes around the world, coupled with formation of mud volcano and brine lake.

Ten-day PENELOPE Cruise in January/February 2007 (KH-06-4 Leg06 survey of the R/V Hakuho-Maru) made detailed mapping and piston/multicores sampling at newly-discovered Medee brine lake and its westward neighboring Medee-Hakuho Mud Volcano (MHMV) in the western branch of the MedRidge. The MHMV has an almost circular dome structure in diameter of ~7km and reaching ~130m high showing very gentle slope, standing on the backstop boundary thrust in water depths of 2260 m. It was initially roughly-recognized during Medee Cruise conducted in 1995 on the basis of its distinct backscatter intensity. The MHMV is interpreted to be active because of existence of many pebbles in the obtained core samples and the high backscattering characteristics.

Little has been clarified the relationship between undergoing collisional tectonics and mud volcanism, although these processes are strongly associated [Kopf 2002]. Mud volcanism in the Eastern Mediterranean Sea is known to be present on contiguous belt along the MedRidge, which is referred to as the "Mediterranean Ridge mud diapiric belt" [Limonov et al. 1996], but mud fields in the western branch of the MedRidge remain poorly solved. This study includes vitrinite reflectance (VR) measurement of the clasts from the pinpoint piston cores obtained from MHMV by means of ROV NSS (Navigable Sampling System), in order to evaluate experienced maximum paleotemperature of the clasts. Some nanofossil ages of the clasts from the MHMV core show ~100 Ma corresponding to the period when Hellenic subduction initiated [Stampfli and Borel 2002]. The subduction system in the eastern Mediterranean has developed dramatically since the period [Ring et al. 2010]. Preliminary results show high VR values suggesting these clasts come from deeper areas as compared with reported results from mud volcano at Kumano Trough [e.g., Muraoka et al. 2011]. Estimating the sediment source and burial depth of MHMV will contribute to qualitatively indicate elevated pore pressure in this subduction zone, or presumably to reveal characterization of the mud volcano coupled with brine lake at the prism-backstop contact.

Keywords: Eastern Mediterranean, Mediterranean Ridge, accretionary prism, mud volcano, vitrinite reflectance

## The source depth of the mud volcano developed in the Kumano Trough

MURAOKA, Satoru<sup>1\*</sup>, ASHI, Juichiro<sup>1</sup>, KANAMATSU, Toshiya<sup>2</sup>, SAKAGUCHI, Arito<sup>2</sup>, AOIKE, Kan<sup>2</sup>, INAGAKI, Fumio<sup>2</sup>

<sup>1</sup>Atmosphere and Ocean Research Institute, <sup>2</sup>JAMSTEC

Submarine mud volcanoes are formed as conical mounds composed of erupted unconsolidated or partially consolidated sediments from mud diapirs which are induced by high pore-fluid pressure and buoyancy developed in the deep underground. Most of them were discovered around subduction zones. Mud diapir that brings deep underground materials to seafloor has an important role for material circulations in subduction zones. Moreover, methane seepages at mound summits are suggested by existences of chemosynthetic biological communities, and accumulation of methane hydrate is expected from core samples and seismic reflection studies. Therefore, mud volcano is also significant in terms of global warming and energy resource.

In order to understand material circulations by mud volcanoes, information about formation mechanism, source layer and its depth is important. In addition, despite mud diapir is generally regarded as rising phenomenon by buoyancy and abnormal high pore pressure, those physical properties are not well investigated. In this study, we discuss the formation mechanism and source depth of mud diapir by using of samples derived from mud volcanoes.

We obtained drilling samples from two sites at the summit of the mud volcano in the Kumano Trough, off Kii Peninsula, SW Japan, during CK09-01 using Deep-Sea Drilling Vessel CHIKYU, in March, 2009. Those sites are near the central part of the vent of the mud volcano.

To understand formation process of mud volcano, anisotropy of magnetic susceptibility, vitrinite reflectance, density, geological description of breccia are conducted. Anisotropy of magnetic susceptibility shows particle arrangement within samples to understand sedimentation and deformation fabrics. While muddy sediments usually exhibit the ellipsoidal body characterized by oblate shape, the samples from the mud volcano show prolate shape rather than oblate shape. Moreover, long axis of the ellipsoidal body shows mostly vertical direction. Therefore, we expected that the drilling site is influenced by vertical material flow.

Porosity of the matrix from the mud volcano is almost constant around 50%. In contrast, the porosity from deposits of the normal basin sediment decreases with the depth and show larger values than those of the mud volcano within 20 m below seafloor. Constant value of porosity of mud volcanoes indicates recent eruption without gravitational compaction. On the other hand, the porosity of breccias shows 20-40%. These values are smaller than those of the surface basin sediment and the matrix of the mud volcano.

Finally, the measured reflectance of vitrinites included in breccias derived from one formation under the seafloor and the age estimated by previous studies give us absolute maximum temperature of breccias. We calculated the depth of one formation by using the value of temperature and the geothermal gradient of this area before mud diapir brought in the formation as breccias. The depth is about 1900 meters under the seafloor. We expect that the source depth of the mud volcano is more depth than 1900 meters depth.

Keywords: mud volcano, mud diapir, vitrinite reflectance, subduction zone, Nankai Trough

## Subduction structure revealed by seismic experiments at the southern Ryukyu Trench

KANEDA, Kentaro<sup>1\*</sup>, NISHIZAWA, Azusa<sup>1</sup>, HORIUCHI, Daishi<sup>1</sup>

<sup>1</sup>Hydrographic and Oceanographic Department, Japan Coast Guard

The Ryukyu Trench (Nansei-Shoto Trench), extending to the east-south of the Ryukyu Arc, is formed by subduction of the Philippine Sea Plate below the Arc. Although great earthquakes have been rarely observed around the Ryukyu Arc and plate coupling at the Ryukyu Trench had been believed to be weak, enormous disasters were induced by earthquakes. Yaeyama Earthquake (M7.4) occurred in 1771 induced large tsunami, which killed more than 11,000 people of the Ryukyu Islands. It is important to determine structure models of a subduction zone to understand mechanism of earthquakes even in a weak plate coupling area.

Although the length of the Ryukyu Trench is longer than the Japan Trench and the Nankai Trough, number of seismic surveys conducted around the Ryukyu Trench to obtain structure models of the subduction is much less than those around the two trenches. Only several structure models of the Ryukyu Trench and the subducting Philippine Sea Plate in shallow area have been constructed until present. In this meeting, we will report a new structure model of the southern Ryukyu Trench at where Japan Coast Guard has been conducted seismic survey.

In 2009, we conducted a seismic reflection experiment with 3,000 m multi-channel streamer cable and a seismic refraction experiment with ocean bottom seismographs (OBSs) on a survey line named ECr5 which runs across the Ryukyu Arc, the Hateruma Basin and the Ryukyu Trench from north to south to the east of the Ishigaki Island. Total volumes of airgun arrays for the reflection and the refraction experiments are 1,050 inch<sup>3</sup> and 6,000 inch<sup>3</sup>, respectively.

To construct a P-wave velocity structure from the OBS records, a ray tracing method with graph theory was used for first arrivals and various reflected signals including reflected signals from the top of the subducting plate and its Moho. A depth scale of the constructed structures was converted to two-way travel time to lay the structure over the multi-channel seismic profile for further interpretation.

Characteristic features of our structure model are follows.

- 1) Backstop structure is located below an edge of the Hateruma Basin.
- 2) Thickness of an accretional prism is thicker than 10 km.
- 3) Approximate subduction angle of the Philippine Sea Plate is 5 degree at shallow (<20 km) part and is 25 degree at deep (20-35 km) part.
- 4) Large fault connecting to the plate boundary at a depth of 15 km reaches to seafloor with an approximate angle of 40 degree.

## The geological structures to the south of the Yaeyama Islands deduced from submarine topography and MCS reflection data

HORIUCHI, Daishi<sup>1\*</sup>, KATO, Yukihiro<sup>1</sup>, NISHIZAWA, Azusa<sup>1</sup>, KANEDA, Kentaro<sup>1</sup>

<sup>1</sup>JHOD, JCG

The Nansei-Shoto Trench is where the Philippine Sea plate is subducting beneath the Eurasian plate. In the southern part of the Nansei-Shoto Trench, the Yaeyama earthquake accompanied a large tsunami killed about 12,000 people in 1771. However, few numbers of structural studies in this region have been carried out compared to those in the Japan Trench and the Nankai Trough regions.

In order to understand characteristics of earthquake occurrence in the Nansei-Shoto Islands, we need the topographical and geological information about Nansei-Shoto Trench.

Japan Coast Guard has been carried out bathymetric, seismic refraction, and multi-channel seismic (MCS) reflection surveys around the Nansei-Shoto Islands. We conducted a seismic survey on an N-S survey line across the forearc basin to the south of the Yaeyama Islands in 2009.

The landward slope of the trench to the south of the Yaeyama Islands is an accretionary wedge with a width of about 50km. To the south of the Yonaguni Island, a linear right-lateral fault with WNW-ESE direction exists at the boundary between the forearc basin and the accretionary wedge (Lallenamd et al.1999.).

On the MCS profile across the right-lateral fault to the southeast of the Ishigaki Island, a flower structure is confirmed around the boundary between the accretionary wedge and the forearc basin. A strong reflector corresponding to a plate boundary is recognized beneath the forearc basin region. This reflector is confirmed to extend to about 50km north from the escarpment at a depth of 20km from the sea surface.

Keywords: Nansei-Shoto trench, Multi-Channel Seismic profile, submarine topography

## Subbottom structures in the region causing the huge tsunami during the 2004 Sumatra-Andaman Earthquake

MISAWA, Ayanori<sup>1\*</sup>, HIRATA, Kenji<sup>2</sup>, Leonard Seeber<sup>3</sup>, Riza Rahardiawan<sup>4</sup>, BABA, Hisatoshi<sup>5</sup>, Katsura Kameo<sup>1</sup>, ADACHI, Keita<sup>1</sup>, SARUKAWA, Hiroshi<sup>5</sup>, UDREKH, Udrek<sup>6</sup>, ARAI, Kohsaku<sup>7</sup>, NAKAMURA, Yasuyuki<sup>8</sup>, KINOSHITA, Masataka<sup>8</sup>, FUJIWARA, Toshiya<sup>8</sup>, ASHI, Juichiro<sup>1</sup>, TOKUYAMA, Hidekazu<sup>1</sup>, Haryadi Permana<sup>9</sup>, Yusuf S. Djajadihardja<sup>10</sup>

<sup>1</sup>AORI, the University of Tokyo, <sup>2</sup>MRI, <sup>3</sup>LDEO, <sup>4</sup>MGI, <sup>5</sup>Tokai University, <sup>6</sup>BPPT, <sup>7</sup>GSJ, AIST, <sup>8</sup>JAMSTEC, <sup>9</sup>LIPI, <sup>10</sup>BAKOSURTANAL

On 26th December 2004, the Sumatra-Andaman Earthquake (Mw 9.2) nucleated offshore northwestern Sumatra Island and then ruptured the megathrust for over ~ 1,300 km mostly to the north along the Sunda Trench. The great tsunami spread over the Indian Ocean and more than the 220,000 people died. Several international marine geological and geophysical surveys have been conducted in this area, especially the Sunda Trench and the Aceh Basin areas. Based on the results from the surveys, five working hypotheses have been proposed for the tsunami source fault model. Among them, Hirata et al. (2008, 2010) suggested that the secondary tsunami source is located around the Middle Thrust of Sibuet et al. (2007). If the 2004 coseismic rupture reached the seafloor along the Middle Thrust, seafloor deformation contributing the great tsunamis would be recorded in the shallow part of the sediment layer.

To image the detailed shallow structure and to map distribution of active faults, we conducted a high-resolution Multi-Channel Seismic (MCS) survey with ship-board Subbottom Profiler (SBP) in the areas during KH-10-5 cruise (using R/V Hakuho-Maru). KH-10-5 MCS survey was carried out in November 2010. Total length of the survey lines was ~484.3 nautical miles. In this MCS survey, a GI gun with a total volume of 150 cubic inch (G: 45 cubic inch, I: 105 cubic inch) and 1200m-long, 48 ch streamer cable were used (steaming at 4 knots, 10 seconds shot interval).

The survey provided fine structural images down to 1.5 sec (TWT) in the trench and to a maximum of 2.0 sec (TWT) in the forearc high region. In the trench region, many landward-vergences (seaward-dipping) faults were identified. These faults reach the seafloor. In general, the trench region seems to suffer active deformation. Additionally, the landward-vergences uplift and deform the oceanic and trench-fill sediments of the Sunda trench. This deformation system has developed the kink folding systems and has also played the role of the accretionary process. In the forearc high area, many of faults and folds were also recognized. A number of ridges in this area are made by many thrust-anticlines. Between the anticline ridges, the syncline and the syncline (or piggyback) basins are also recognized. The sedimentary layers of syncline basins can be usually imaged down to a maximum of 0.5 sec (TWT) below the seafloor. In the deep part of these basins, sediment is often tilted landward. These tilted layers form a proto-deformation related to the shortening of the forearc and the development of the anticline ridges. In contrast, the shallow part of these basins is mostly flat-lying and laterally coherent. It indicates that the recently deformation activity of this area is relatively low. Along the Middle thrust, however, we found evidence in both MCS and SBP data of recent deformation in the near-surface layer. This active deformation area is almost coincident with the position of the predicted secondary tsunami source fault predicted by Hirata et al. (2008). However, only the high-resolution MCS and shipboard SBP data alone cannot decide if this deformation was activated coseismically during the 2004 event. Also, the deeper structure of the Middle Thrust could not be recovered by our MCS data. Additional survey will be required, such as the high-resolution deep-tow SBP and piston coring will be required in near future as well as a large-scale MCS survey with larger volume air-gun and much long streamer.

Keywords: 2004 Sumatra-Andaman Earthquake, Tsunami, Subbottom structure, High-resolution Multi-Channel Seismic survey